

The aryl hydrocarbon receptor in β -cells mediates the effects of TCDD on glucose homeostasis in mice



Myriam P. Hoyeck¹, Ma. Enrica Angela Ching¹, Lahari Basu¹, Kyle van Allen¹, Jana Palaniyandi¹, Ineli Perera¹, Emilia Poleo-Giordani¹, Antonio A. Hanson¹, Peyman Ghorbani², Morgan D. Fullerton^{2,3}, Jennifer E. Bruin^{1,*}

ABSTRACT

Objective: Chronic exposure to persistent organic pollutants (POPs) is associated with increased incidence of type 2 diabetes, hyperglycemia, and poor insulin secretion in humans. Dioxins and dioxin-like compounds are a broad class of POPs that exert cellular toxicity through activation of the aryl hydrocarbon receptor (AhR). We previously showed that a single high-dose injection of 2,3,7,8-tetrachlorodibenzo-*p*-dioxin (TCDD, aka dioxin; 20 $\mu\text{g}/\text{kg}$) *in vivo* reduced fasted and glucose-stimulated plasma insulin levels for up to 6 weeks in male and female mice. TCDD-exposed male mice were also modestly hypoglycemic and had increased insulin sensitivity, whereas TCDD-exposed females were transiently glucose intolerant. Whether these effects are driven by AhR activation in β -cells requires investigation.

Methods: We exposed female and male β -cell specific *Ahr* knockout ($\beta\text{Ahr}^{\text{KO}}$) mice and littermate *Ins1-Cre* genotype controls ($\beta\text{Ahr}^{\text{WT}}$) to a single high dose of 20 $\mu\text{g}/\text{kg}$ TCDD and tracked the mice for 6 weeks.

Results: Under baseline conditions, deleting AhR from β -cells caused hypoglycemia in female mice, increased insulin secretion *ex vivo* in female mouse islets, and promoted modest weight gain in male mice. Importantly, high-dose TCDD exposure impaired glucose homeostasis and β -cell function in $\beta\text{Ahr}^{\text{WT}}$ mice, but these phenotypes were largely abolished in TCDD-exposed $\beta\text{Ahr}^{\text{KO}}$ mice.

Conclusion: Our study demonstrates that AhR signaling in β -cells is important for regulating baseline β -cell function in female mice and energy homeostasis in male mice. We also show that β -cell AhR signaling largely mediates the effects of TCDD on glucose homeostasis in both sexes, suggesting that the effects of TCDD on β -cell function and health are driving metabolic phenotypes in peripheral tissues.

© 2024 The Authors. Published by Elsevier GmbH. This is an open access article under the CC BY-NC-ND license (<http://creativecommons.org/licenses/by-nc-nd/4.0/>).

Keywords Aryl hydrocarbon receptor; β -cells; Cre-loxP knockout; Type 2 diabetes; Dioxins; Environmental pollutants

1. INTRODUCTION

Persistent organic pollutants (POPs) are a diverse family of lipophilic environmental contaminants that resist degradation, leading to their widespread global dispersion. Chronic exposure to POPs is associated with numerous adverse health outcomes in humans, including increased risk of type 2 diabetes (T2D) [1–7], hyperglycemia [1,7–11] and poor insulin secretion [1,10–14]. However, the causal link between POP exposure and metabolic dysregulation remains poorly understood. Dioxins and dioxin-like compounds are a broad class of POPs that exert cellular toxicity through activation of the aryl hydrocarbon receptor (AhR). AhR is a ligand-dependent nuclear receptor that is involved in numerous biological processes. The canonical AhR pathway is involved in the detoxification of xenobiotic compounds (such as dioxins) via activation of phase I (e.g. cytochrome P450, CYP450) and phase II (e.g. NAD(P)H: quinone oxidoreductase, NQO1; glutathione S-transferase alpha 1, GSTA1) xenobiotic metabolism enzymes [15,16]; however,

activation of these enzymes can also lead to oxidative stress and consequently DNA damage. Global and tissue-specific AhR knockout models have also revealed an essential role of AhR in non-canonical processes, including cell proliferation and adhesion, apoptosis, protein degradation, organ development, immune responses, and circadian rhythms [16–20]. Importantly, global AhR knockout mice have increased insulin sensitivity and improved glucose tolerance on both chow [21] and high-fat diets (HFD) [22], and reduced adiposity when fed a HFD [22], implicating AhR in regulating energy metabolism and glucose homeostasis.

Our lab has shown that direct *in vitro* and systemic *in vivo* exposure to the AhR ligand, 2,3,7,8-tetrachlorodibenzo-*p*-dioxin (TCDD, aka “dioxin”), induced *Cyp1a1* gene expression in mouse pancreatic islets [23–25]. This indicates that dioxins directly activate AhR within the endocrine pancreas, but the impact of AhR signaling on β -cell function remains unclear. We have shown that a single high-dose injection of TCDD (20 $\mu\text{g}/\text{kg}$) *in vivo* reduced fasted and glucose-stimulated plasma

¹Department of Biology & Institute of Biochemistry, Carleton University, Ottawa, ON, Canada ²Department of Biochemistry, Microbiology and Immunology, Faculty of Medicine, Centre for Infection, Immunity and Inflammation, Ottawa Institute of Systems Biology, Ottawa, ON, Canada ³Centre for Catalysis Research and Innovation, University of Ottawa, Ottawa, ON, Canada

*Corresponding author. E-mail: jenny.bruin@carleton.ca (J.E. Bruin).

Received November 13, 2023 • Revision received January 24, 2024 • Accepted January 30, 2024 • Available online 2 February 2024

<https://doi.org/10.1016/j.molmet.2024.101893>

Abbreviations

| | |
|--------------|--|
| AhR | Aryl hydrocarbon receptor |
| CO | Corn oil |
| Cyp1a1 | Cytochrome P450 1A1 |
| GTT | Glucose tolerance test |
| GSIS | Glucose-stimulated insulin secretion |
| Gsta1 | Glutathione S-transferase alpha 1 |
| Il-1 β | Interleukin-1 β |
| ITT | Insulin tolerance test |
| Nqo1 | NAD(P)H: quinone oxidoreductase |
| POPs | Persistent organic pollutants |
| Ppargc1a | Peroxisome proliferative activated receptor 1 α |
| TCDD | 2,3,7,8-tetrachlorodibenzo- <i>p</i> -dioxin |
| T2D | Type 2 diabetes |

insulin levels for up to 6 weeks in male and female mice [24]. TCDD-exposed male mice were also modestly hypoglycemic and had increased insulin sensitivity, whereas TCDD-exposed females were transiently glucose intolerant compared to CO-exposed mice. It is unclear if the direct action of TCDD on β -cells contributes to these sex-specific metabolic outcomes. Interestingly, high-dose TCDD exposure did not reduce plasma insulin levels in male mice with a global AhR deletion [26], supporting a role of AhR in mediating the effects of TCDD *in vivo*; whether this is driven by the AhR pathway in β -cells requires investigation.

To elucidate the role of AhR in β -cells, we generated a β -cell specific *Ahr* knockout (β Ahr^{KO}) mouse model using the Cre-loxP system. We first assessed the role of β -cell AhR in regulating body weight, glucose homeostasis, and β -cell health in the absence of exogenous chemical stimuli. We then administered a single high-dose of TCDD (20 μ g/kg), as in our previous study [24], to determine whether the effects of TCDD on glucose homeostasis and β -cell function/health in mice are mediated by β -cell AhR signaling. We report that deleting *Ahr* from β -cells promoted modest weight gain in male mice, caused hypoglycemia in female mice, and increased insulin secretion in isolated female islets *ex vivo* under baseline conditions. Importantly, high-dose TCDD exposure impaired glucose homeostasis and β -cell function in β Ahr^{WT} mice (*Ins1-Cre* genotype control), but these phenotypes were largely abolished in TCDD-exposed β Ahr^{KO} mice. Collectively, our study demonstrated that AhR signaling in β -cells mediates the effects of TCDD on glucose homeostasis in both female and male mice, most likely by promoting β -cell dysfunction.

2. MATERIALS AND METHODS

2.1. Animals

All mice received *ad libitum* access to standard rodent chow (Harlan Laboratories, Teklad Diet #2018; Madison, WI) and were maintained on a 12-hour light/dark cycle throughout the study. All experiments were approved by the Carleton University Animal Care Committee and carried out in accordance with the Canadian Council on Animal Care guidelines. Prior to beginning experimental protocols, animals were randomly assigned to treatment groups and matched for body weight and blood glucose to ensure that these variables were consistent between groups.

2.1.1. Generating β -cell specific *Ahr* knockout mice

B6(Cg)-*Ins1*^{tm3.1Bra¹J} (#026801; mice expressing Cre recombinase under the control of the *insulin-1* (*Ins-1*) promoter; Supplemental

Figure 1C) and *Ahr*^{tm3.1Bra¹J} (#006203; mice with loxP sites flanking exon 2 of the *Ahr* allele; Supplemental Figure 1B) were purchased from The Jackson Labs (Bar Harbour, ME, USA). These mice were crossed to generate mice with a partial *Ahr* knockout in β -cells (β Ahr^{fl/+} *Ins1*^{Cre/+}), which were further crossed to generate β Ahr^{fl/fl} *Ins1*^{+/+} and β Ahr^{fl/+} *Ins1*^{Cre/Cre} mice. Our experimental mice were then generated by crossing β Ahr^{fl/+} *Ins1*^{+/+} females with β Ahr^{fl/+} *Ins1*^{Cre/Cre} males. We refer to β -cell specific *Ahr* knockout mice (β Ahr^{fl/fl} *Ins1*^{Cre/+}) as “ β Ahr^{KO}” and genotype control mice with a single copy of *Ins1-Cre* (β Ahr^{+/+} *Ins1*^{Cre/+}) as “ β Ahr^{WT}” (Supplemental Figure 1A). Genotypes were confirmed by PCR from an ear notch using iProof HF master mix (Biorad, #1725310; Mississauga, ON, Canada) and primer sequences provided by The Jackson Labs, and subsequently running PCR products on a 2 % agarose gel (Supplemental Figure 1B,C; primer sequences in Supplemental Table 1).

2.1.2. Validating β -cell specific *Ahr* knockout mice

We confirmed deletion of *Ahr* by verifying that recombination was occurring along exon 2 of the *Ahr* gene in whole islets, dispersed islets, and sorted β -cells. Islets were isolated from β Ahr^{WT} and β Ahr^{KO} mice at 15–55 weeks of age, as described in Section 2.3. A subset of whole islets was stored in buffer RLT with 1 % β -mercaptoethanol for qPCR analysis (~70 islets/biological replicate, n = 6–7 biological replicates/group). Another subset of islets was dispersed, sorted to collect a pure β -cell population, as described in Section 2.4, and subsequently stored in TRIzolTM (Invitrogen, #15596018; Carlsbad, CA, USA) for qPCR analysis. Liver was harvested from β Ahr^{WT} and β Ahr^{KO} mice at 33–41 weeks of age and flash frozen (n = 9 biological replicates/group) for qPCR analysis.

Ahr primers were designed to bind on either side of exon 2 or within exon 2 to assess recombination at exon 2 (Supplemental Figure 1D, primer sequences in Supplemental Table 2). *Ahr* was amplified in whole islets, dispersed islets, and sorted β -cells using qPCR with primers for both the outside and inside of exon 2, and gene products were run on a 2 % agarose gel. The same method was used to ensure that no *Ahr* recombination was occurring in liver of β Ahr^{KO} mice.

2.1.3. *In vivo* TCDD-exposure study protocol

Female and male β Ahr^{KO} and β Ahr^{WT} mice were generated as described in Section 2.1.1; 45 litters were generated, with ~58 % of litters having both β Ahr^{KO} mice and corresponding β Ahr^{WT} littermate controls. At 6–37 weeks of age, β Ahr^{KO} and β Ahr^{WT} mice received a single intraperitoneal (i.p.) injection of corn oil (CO; 25 ml/kg, vehicle control, Sigma-Aldrich, #C8267-2.5L; St Louis, MO, USA) or 20 μ g/kg TCDD (AccuStandard, #AD404SDMS010X), as outlined in Figure 2A (n = 17–21 mice/group). At 1-week post-injection, islets were isolated from a subset of mice for an *ex vivo* glucose-stimulated insulin secretion (GSIS) assay, cell viability assessment, and RNA extraction (n = 6–7 mice/group); liver was extracted from the same subset of mice and flash frozen for qPCR analysis (n = 6–7 mice/group). Whole pancreas was harvested from another subset of mice at 1-week post-injection and stored in 4 % paraformaldehyde (PFA) for 24 h, followed by long-term storage in 70 % ethanol for histological analysis (n = 5–7 mice/group). At 6 weeks post-injection, islets were isolated from a third subset of mice for an *ex vivo* GSIS assay and RNA extraction. All tissues were harvested from random-fed mice.

2.2. Metabolic assessments

All metabolic analyses were performed in conscious, restrained mice, and blood samples were collected via the saphenous vein using heparinized microhematocrit tubes (Fisherbrand, #22-362-566). Blood

glucose levels were measured using a handheld glucometer (Medi-Sure; Ajax, Canada). Body weight and blood glucose were measured following a 4-h morning fast 1–2x/week throughout the study. For all metabolic tests, time 0 indicates the blood sample collected prior to administration of glucose or insulin. For glucose tolerance tests (GTTs), mice received an i.p. bolus of glucose (2 g/kg) following a 6-h morning fast. Blood samples were collected at 0, 15, 30, and 60 min for measuring plasma insulin levels by ELISA (ALPCO, #80-INSMU-E01; Salem, NH, USA). GTTs were conducted at 1-, 4- and 6-weeks post CO or TCDD injection. For insulin tolerance tests (ITTs), mice received an i.p. bolus of insulin (0.7 IU/kg; Novolin ge Toronto, #02024233; Novo Nordisk, Canada) following a 4-h morning fast. An ITT was performed at 1–2 weeks post CO or TCDD injection.

2.3. Islet isolation

Islets were isolated by pancreatic duct injection with collagenase (1,000 units/ml; Sigma Aldrich, #C7657) dissolved in Hanks' balanced salt solution (HBSS: 137 mM NaCl, 5.4 mM KCl, 4.2 mM NaH₂PO₄, 4.1 mM KH₂PO₄, 10 mM HEPES, 1 mM MgCl₂, 5 mM dextrose, pH 7.2). Pancreata were incubated at 37 °C for 10 min 45 sec, vigorously agitated, and the collagenase reaction quenched by adding cold HBSS with 1 mM CaCl₂. Pancreas tissue was washed 3 times in HBSS + CaCl₂ (centrifuging for 1 min at 1000 rpm between washes) and resuspended in RPMI 1640 1X (Wisent Bioproducts, 350-000-CL; St-Bruno, Canada) containing 10 % fetal bovine serum (FBS; Sigma-Aldrich, #F1051-500 ml) and 1 % 10000 IU/ml penicillin-streptomycin (Gibco, #15140-122-100). Pancreas tissue was filtered through a 70 µm cell strainer and islets were handpicked under a dissecting scope to >95 % purity. The day following isolation, islets were used for cell sorting, *ex vivo* GSIS, cell viability assessment, or stored in buffer RLT with 1 % β-mercaptoethanol for RNA extraction.

2.4. Fluorescence-activated cell sorting (FACS)

To sort islets, 400–600 islets per replicate (n = 3 biological replicates/group) were transferred to a 1.5 mL microcentrifuge tube and washed with pre-warmed PBS+/+ (Sigma, #D8662) [27]. Islets were dispersed by adding 400 µl Accutase (VWR, CA10215-416) and incubating islets at 37 °C for ~4–6 min with trituration occurring every 2 min (VWR, #CA10215-416). Accutase was neutralized with 600 µl RPMI 1640 + 10 % FBS + 1 % 10000 IU/ml penicillin-streptomycin. Cells were incubated in blocking solution (PBS + 2 % FBS) for 5 min at room temperature. Cells were incubated in 50 µl primary antibody mixture (antibody information below) for 15 min at room temperature. Cells were washed with 1 mL of PBS + 2 % FBS and then incubated in 50 µl secondary antibody (antibody information below) for 20 min at room temperature. Next, 50 µl of 2.8 µM DAPI + 4 mM EDTA was added to each sample just prior to sorting. Samples were sorted on a SH800S Cell Sorter (Sony).

Cells were gated based on size, granularity, and geometry for singlets (Supplemental Figure 1E) [27]. Cells negative for DAPI and TER-119-biotin (erythroid cell marker; BioLegend, #133307; San Diego, CA, USA), CD31-biotin (endothelial cell marker; BioLegend, #102503), and CD45-biotin (hematopoietic cell marker; BioLegend, #103101) detected by streptavidin-BV421 (1:200, BioLegend, #405226) in the FL-1 channel and positive for EpCAM-PerCP/Cy5.5 (endocrine cell marker; BioLegend, #118219) in the FL-5 channel were gated. Endocrine cells were further sorted by CD24-APC⁺ve (δ-cell marker; BioLegend, 138505) δ-cells and CD24^{-ve} cells on FL-4. CD24^{-ve} cells were further gated into CD71⁺ve (β-cell marker; BioLegend, #113805) and CD49f⁺ve cells (β-cell marker; BioLegend, #313611) on FL-2 and FL-3, respectively, to exclude α-cells. β-cells were collected in a

1.5 mL microcentrifuge tube containing 50 µl FBS and immediately resuspended in Trizol and stored at –20 °C until RNA extraction [27]. Additional details on antibodies are included in Supplemental Table 4.

2.5. *Ex vivo* glucose-stimulated insulin secretion assay

To assess β-cell function, 25 islets per replicate (n = 3 technical replicates/mouse; n = 3–8 mice/group) were transferred to a 1.5 mL microcentrifuge tube and washed with pre-warmed (37 °C) Krebs–Ringer bicarbonate buffer (KRBB) with 0 mM glucose (115 mM NaCl, 5 mM KCl, 24 mM NaHCO₃, 2.5 mM CaCl₂, 1 mM MgCl₂, 10 mM HEPES, 0.1 % (wt/vol.) BSA, pH 7.4). Islets were then immersed in KRBB with 2.8 mM glucose (low glucose, LG) for a 1 h pre-incubation at 37 °C and the supernatant was discarded. Islets were then immersed in 500 µl of LG KRBB for 1 h, followed by 500 µl of KRBB with 16.7 mM glucose (high glucose, HG) for 1 h at 37 °C. The LG KRBB and HG KRBB samples were centrifuged (2000 rpm) and the supernatant stored at –30 °C until use. To measure insulin content, islets were immersed in 500 µl of acid-ethanol solution (1.5 % (vol./vol.) HCl in 70 % (vol./vol.) ethanol) at 4 °C overnight and then neutralised with 1 M Tris base (pH 7.5) before long-term storage at –30 °C. Insulin concentrations were measured by ELISA (ALPCO, #80-INSMR).

2.6. Islet cell viability

To assess cell viability, 50 islets per replicate (n = 2 technical replicates/mouse; n = 3–9 mice/group) were transferred to a 1.5 mL microcentrifuge tube and dispersed as described in Section 2.4. Following dispersing, cells were washed once with PBS+/+ and then stained with 0.5 µM Hoescht (Thermo Scientific, #62249), 1.25 µM Calcein (Invitrogen, #L3224), and 0.75 µM PI (Invitrogen, #P21493) at room temperature for 30 min in a 96-well flat-bottom plate pre-coated with poly-D-lysine (Sigma-Aldrich #P7280). An Axio Observer 7 microscope was used to image 10 % of each well immediately after staining. The number of calcein⁺ cells (live) and PI⁺ cells (dead/dying) was quantified using Zen Blue 2.6 software (Carl Zeiss, Germany). The % live cell was calculated as [(# of live cells imaged in well)/(total # cell imaged in well) * 100], with an average of 1650 cells counted per well.

2.7. Quantitative real time PCR

RNA was extracted from isolated islets stored in buffer RLT with 1 % β-mercaptoethanol using the Qiagen RNeasy Micro Kit (#74004). RNA was extracted from flash frozen liver using TRIzolTM (Invitrogen, #15596018; Carlsbad, CA, USA), as per the manufacturer's instructions. DNase treatment was performed prior to cDNA synthesis with the iScriptTM gDNA Clear cDNA Synthesis Kit (Biorad, #1725035). qPCR was performed using SsoAdvanced Universal SYBR Green Supermix (Biorad, #1725271) and run on a CFX384 (Biorad). *PPIA* was used as the reference gene since this gene displayed stable expression under control and treatment conditions. Data were analyzed using the 2^{–ΔΔCT} relative quantitation method. Primer sequences are listed in Supplemental Table 1–3.

2.8. Immunofluorescence staining and image quantification

PFA-fixed pancreas tissues were processed and paraffin-embedded by the University of Ottawa Heart Institute Histology Core Facility (Ottawa, ON). Immunofluorescent staining was performed on tissue sections (5 µm thick), as previously described [23]. Apoptosis was assessed using the Molecular Probes Click-It Plus TUNEL Assay with Alexa Fluor 488 dye (Invitrogen, #C10617), according to manufacturer's instructions. Pancreas sections were counterstained with rabbit anti-insulin (1:200, C27C9; Cell Signaling Technology, #3014, Danvers,

MA, USA) and goat anti-rabbit IgG (H + L) secondary antibody, Alexa Fluor 594 (1:1000; Invitrogen, #A11037) with no antigen retrieval. For every round of staining, a pancreas section was treated with DNase (Qiagen, # 1023460) prior to TUNEL staining as a positive control. Macrophage infiltration into islets was assessed by staining pancreas tissues with rat anti-F4/80 (1:100; CedarLane, #CL8940AP; Burlington, ON, Canada) and mouse anti-insulin (1:250; L6B10, Cell Signaling, # 8138S); secondary antibodies used included goat anti-rat IgG (H + L) Alexa Fluor 594 (1:1000; Invitrogen, #A11007) and goat anti-mouse IgG (H + L) Alexa Fluor 488 (1:1000; Invitrogen, #A11029). A section of adipose tissue from a HFD-fed mouse was included as a positive control for F4/80 immunoreactivity.

For islet morphology quantification, the entire pancreas section was imaged with an Axio Observer 7 microscope and all islets within the field of view were quantified. The average of all islet measurements is reported for each biological replicate. The % INS^{+ve} area per islet was calculated as [(hormone^{+ve} area/islet area) x 100], with a range of 2–8 islets quantified per mouse. Immunofluorescence was manually quantified using Zen Blue 2.6 software. The % TUNEL^{+ve} INS^{+ve} cells per pancreas section was calculated as [(# of TUNEL^{+ve} INS^{+ve} cells per pancreas section)/(total # of INS^{+ve} cells per pancreas section) x 100], with an average of 350 cells counted per pancreas section.

2.9. Quantification and statistical analysis

All statistics were performed using GraphPad Prism 10.1.0 (GraphPad Software Inc., La Jolla, CA). Specific statistical tests are indicated in figure legends. Sample sizes are described in Section 2.1 and in figure legends. For all analyses, $p \leq 0.05$ was considered statistically significant. Statistically significant outliers were detected by a Grubbs' test with $\alpha = 0.05$. All data was tested for normality using a Shapiro-Wilk test and for equal variance using either a Brown–Forsyth test (for one-way ANOVAs) or an F test (for unpaired t-tests). Non-parametric statistics were used in cases where the data failed normality or equal variance tests. Parametric tests were used for all two-way ANOVAs, but normality and equal variance were tested on area under the curve (AUC) values and by one-way ANOVAs. Data in line and bar graphs display mean \pm SEM. Individual data points on bar plots are always biological replicates (i.e. different mice).

3. RESULTS

3.1. Validation and characterization of β Ahr^{KO} mice

Our breeding scheme involved crossing Ahr^{+/+} Ins^{Cre/Cre} and Ahr^{fl/fl} Ins^{+/+} mice to generate heterozygous Ahr^{fl/+} Ins^{Cre/+} mice, which were then crossed to each other to generate Ahr^{fl/+} Ins^{Cre/Cre} and Ahr^{fl/+} Ins^{+/+} mice (Supplemental Figure 1A). These mice were further crossed to generate Ahr^{+/+} Ins^{Cre/+} (“ β Ahr^{WT}”) and Ahr^{fl/fl} Ins^{Cre/+} (“ β Ahr^{KO}”) littermates (Supplemental Figure 1A).

We first validated our β Ahr^{KO} model by assessing recombination along exon 2 of the *Ahr* gene in liver and whole islets by qPCR analysis. A single *Ahr* product band (263 base pairs, bp) was observed in β Ahr^{WT} liver (Supplemental Figure 1F) and β Ahr^{WT} whole islets (Supplemental Figure 1G), indicating the presence of exon 2. As expected, β Ahr^{KO} mice had a truncated *Ahr* gene product (76 bp) in whole islets (Supplemental Figure 1G) but not liver (Supplemental Figure 1F), confirming that *Ahr* recombination is specific to islets. The presence of a full-length *Ahr* gene product in β Ahr^{KO} islets (Supplemental Figure 1G) was expected given that islets are a mixture of β -cells and other endocrine cells. As such, we next assessed whether recombination was occurring specifically in β -cells by comparing *Ahr* expression in whole islets, dispersed islets, and sorted β -cells. We

observed a full-length *Ahr* in β Ahr^{WT} whole islets, dispersed islets, and sorted β -cells (Supplemental Figure 1H) and confirmed the presence of *Ahr* exon 2 (Supplemental Figure 1I). We again show that whole and dispersed β Ahr^{KO} islets had both a full-length and truncated *Ahr* gene (Supplemental Figure 1H). Importantly, sorted β -cells from β Ahr^{KO} islets only had a truncated *Ahr* gene (Supplemental Figure 1H), which lacked exon 2 (Supplemental Figure 1I), confirming that *Ahr* was successfully deleted from β -cells.

Next, we assessed whether *Ahr* deletion in β -cells impacted metabolic health under baseline conditions (i.e. in the absence of exogenous chemical exposure). β Ahr^{KO} females had normal body weight between 6 and 11 weeks of age (Figure 1A) and normal fasted plasma insulin levels at 9.5–14 weeks (Figure 1C), but displayed a significant decrease in fasted blood glucose levels at 6 and 10 weeks (Figure 1B) compared to β Ahr^{WT} females. There was no overall effect of genotype on fasted blood glucose (Figure 1E) or plasma insulin levels (Figure 1F) in male mice. Interestingly, β Ahr^{KO} males had significantly higher body weight compared to β Ahr^{WT} males at both 8 and 12 weeks of age (Figure 1D). These data suggest that AhR signaling in β -cells plays a role in maintaining metabolic health under baseline conditions.

3.2. Deleting *Ahr* from β -cells protected TCDD-exposed female mice from transient hypoglycemia

We next assessed whether AhR in β -cells mediates the effects of TCDD on glucose homeostasis and β -cell function. Male and female β Ahr^{WT} and β Ahr^{KO} mice were exposed to CO or a single high dose of TCDD (20 μ g/kg) and tracked for up to 6 weeks post-injection (Figure 2A). TCDD exposure had no effect on body weight in female mice (Figure 2B,C), or body weight (Figure 2F,G) and fasting blood glucose (Figure 2H,I) in male mice, irrespective of genotype. Interestingly, TCDD caused transient hypoglycemia 1-day post-injection in β Ahr^{WT} but not β Ahr^{KO} females (Figure 2D,E). β Ahr^{KO} males continued to display higher body weight than β Ahr^{WT} males throughout the 6-week study, irrespective of chemical exposure (Figure 2G).

3.3. Deletion of *Ahr* in β -cells protected female and male mice from TCDD-induced changes in glycemia

To determine the impact of β -cell AhR on regulating glucose homeostasis following TCDD exposure, we performed ipGTTs at 1-, 4-, and 6-weeks post CO or TCDD injection. TCDD exposure had no overall effect on glucose tolerance in β Ahr^{WT} or β Ahr^{KO} females at 1-week post-injection (Figure 3A,B). By 4 weeks post-injection, TCDD-exposed β Ahr^{WT} females had modest glucose intolerance (Figure 3Cii), which became more pronounced by 6 weeks post-injection (Figure 3Eii,F). In contrast, TCDD-exposed β Ahr^{KO} females maintained normal glycemia relative to CO-exposed females at both week 4 and 6 (Figure 3Ciii,D,Eiii,F).

TCDD-exposed β Ahr^{WT} males were significantly hypoglycemic compared to CO-exposed β Ahr^{WT} males at 1-week post-injection (Figure 3Gii), but normoglycemia was restored by 4 weeks (Figure 3I-L). In contrast, TCDD exposure had no effect on glucose tolerance in β Ahr^{KO} males at any timepoint (Figure 3Giii-Kiii). These data imply that AhR signaling in β -cells mediates the effects of TCDD on glucose homeostasis.

3.4. Deleting *Ahr* in β -cells delayed the onset of glucose-induced hypoinsulinemia in TCDD-exposed male mice

Consistent with the GTT data, TCDD exposure had no overall effect on plasma insulin levels in females of either genotype at 1-week (Figure 4A,B) or 4 weeks (Figure 4C,D) post-injection. However, by 6 weeks, TCDD-exposed β Ahr^{WT} females displayed a modest and

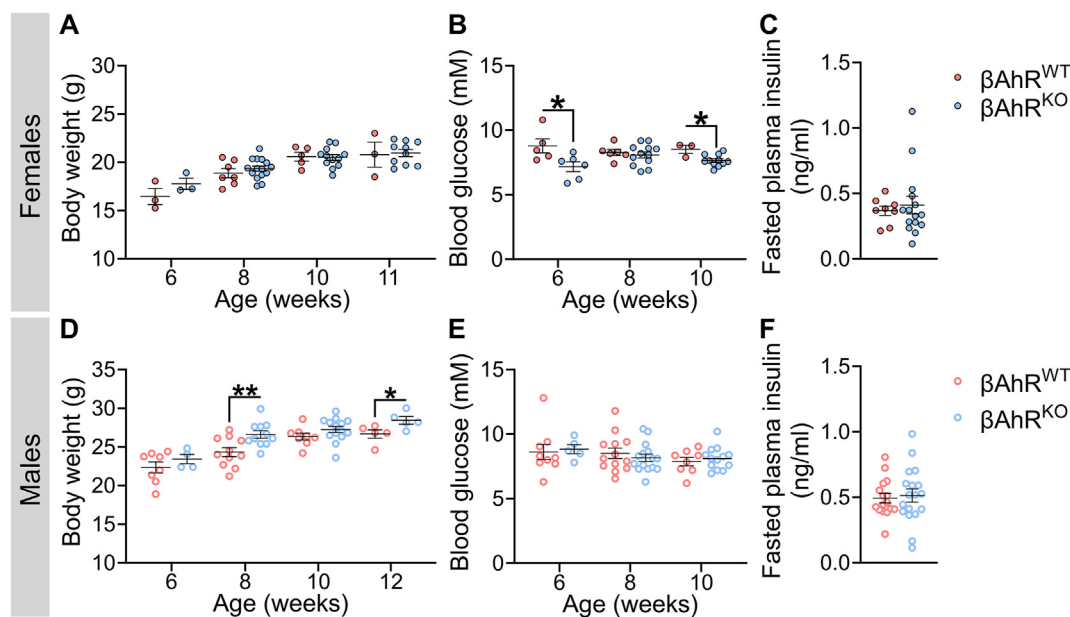


Figure 1: Deleting *Ahr* in β -cells caused hypoglycemia in females and increased body weight in males under baseline condition. Mice were 6–12 weeks old when tracking was started. All tracking data was collected prior to chemical administration. (A,D) Body weight, (B,E) fasted blood glucose, and (C,F) fasted plasma insulin in (A–C) female and (D–F) male β Ahr^{WT} and β Ahr^{KO} mice. All data are presented as mean \pm SEM. Individual data points on bar graphs represent biological replicates (different mice). * $p \leq 0.05$. The following statistical tests were used: (A–F) two-tailed unpaired t-test at each individual time point.

trending decrease in plasma insulin levels (Figure 4Eii,F), which was not observed in β Ahr^{KO} females (Figure 4Eiii,F).

TCDD exposure caused severe hypoinsulinemia in β Ahr^{WT} males compared to CO-exposed β Ahr^{WT} males at 1-week post-exposure (Figure 4Gii,H), with the severity of hypoinsulinemia diminishing over time (Figure 4Iii,J,Kii,L). This phenotype was largely abolished by knocking out *Ahr* in β -cells, with TCDD-exposed β Ahr^{KO} males only displaying modest hypoinsulinemia at 6 weeks post-exposure (Figure 4G–L). In summary, our GTT data shows that *Ahr* deletion in β -cells had little to no effect on glucose homeostasis or glucose-stimulated plasma insulin levels in female and male mice exposed to corn oil. However, β -cell AhR plays a clear role in the metabolic response to an exogenous AhR ligand.

3.5. β Ahr^{KO} female and male mice were protected from TCDD-induced changes in insulin sensitivity

We previously reported that TCDD-exposed male WT mice were more insulin sensitive than CO-exposed males [24]. Since changes in insulin secretion can drive adaptations in peripheral sensitivity [28,29], we examined whether β -cell *Ahr* deletion mitigated the effects of TCDD on insulin sensitivity (Figure 5A,B,E,F). In β Ahr^{WT} females, TCDD exposure caused a modest increase in insulin sensitivity at 15-min post-insulin, followed by insulin resistance at 60- and 90-min post-insulin compared to CO-injected controls (Figure 5Aii); this effect was largely absent in TCDD-exposed β Ahr^{KO} females (Figure 5Aiii). TCDD-exposed β Ahr^{WT} males were significantly more insulin sensitive throughout the ITT compared to CO-exposed β Ahr^{WT} males (Figure 5Eii), whereas TCDD had no effect on insulin sensitivity in β Ahr^{KO} males (Figure 5Eiii).

The ITT results suggest a role for β -cell AhR signaling in driving the effects of TCDD on peripheral tissues. To further explore this idea, we measured gene expression for markers of the AhR pathway and insulin signaling in liver tissue from β Ahr^{WT} and β Ahr^{KO} mice (Figure 5C,D,G,H). There were no changes in liver *Ahr* expression, irrespective of genotype

or chemical exposure (Figure 5C,G). Interestingly, *Cyp1a1*, *Nqo1*, and *Gsta1* expression were significantly upregulated in liver of TCDD-exposed β Ahr^{WT} and β Ahr^{KO} mice compared to CO-exposed mice, but expression was dampened in TCDD-exposed β Ahr^{KO} liver compared to β Ahr^{WT} liver (Figure 5C,G), despite the absence of *Ahr* recombination in the liver (Supplemental Figure 1F).

TCDD exposure also reduced expression of the gluconeogenesis enzyme *G6pc* (glucose-6-phosphatase) in liver from β Ahr^{WT} female (Figure 5D) and male (Figure 5H) mice compared to CO exposure, an effect that was absent in β Ahr^{KO} mice (Figure 5D,H). Similarly, the lipogenesis markers *Acaca* (acetyl-CoA carboxylase alpha; Figure 5H) and *Ppargc1a* (peroxisome proliferator-activated receptor gamma coactivator 1-alpha; Figure 5H) was reduced in TCDD-exposed β Ahr^{WT} males compared to CO-exposed β Ahr^{WT} males, but *Ahr* deletion in β -cells prevented this effect. In contrast, TCDD reduced expression of the gluconeogenesis enzyme *Pck1* (phosphoenolpyruvate carboxykinase 1) in female (Figure 5D) and male (Figure 5H) liver, irrespective of genotype. There was no effect of chemical or genotype on liver *Acaca* or *Ppargc1a* expression in females (Figure 5D). Collectively, these data suggest that the effects of TCDD on β -cell physiology are driving changes in peripheral insulin sensitivity, most likely due to AhR-mediated changes in insulin secretion.

3.6. TCDD exposure impaired insulin secretion *ex vivo* in β Ahr^{WT} but not β Ahr^{KO} male islets

Next, we assessed whether AhR signaling in β -cells impacts β -cell function by measuring GSIS in isolated islets *ex vivo* at 1- and 6 weeks following CO or TCDD injection. Interestingly, β Ahr^{KO} female islets showed increased basal insulin secretion under LG conditions compared to β Ahr^{WT} islets (Figure 6B,F). β Ahr^{KO} female islets also had increased insulin secretion under high-glucose condition compared to β Ahr^{WT} islets at week 6 (Figure 6E), pointing to a role of AhR in regulating β -cell function in female mouse islets.

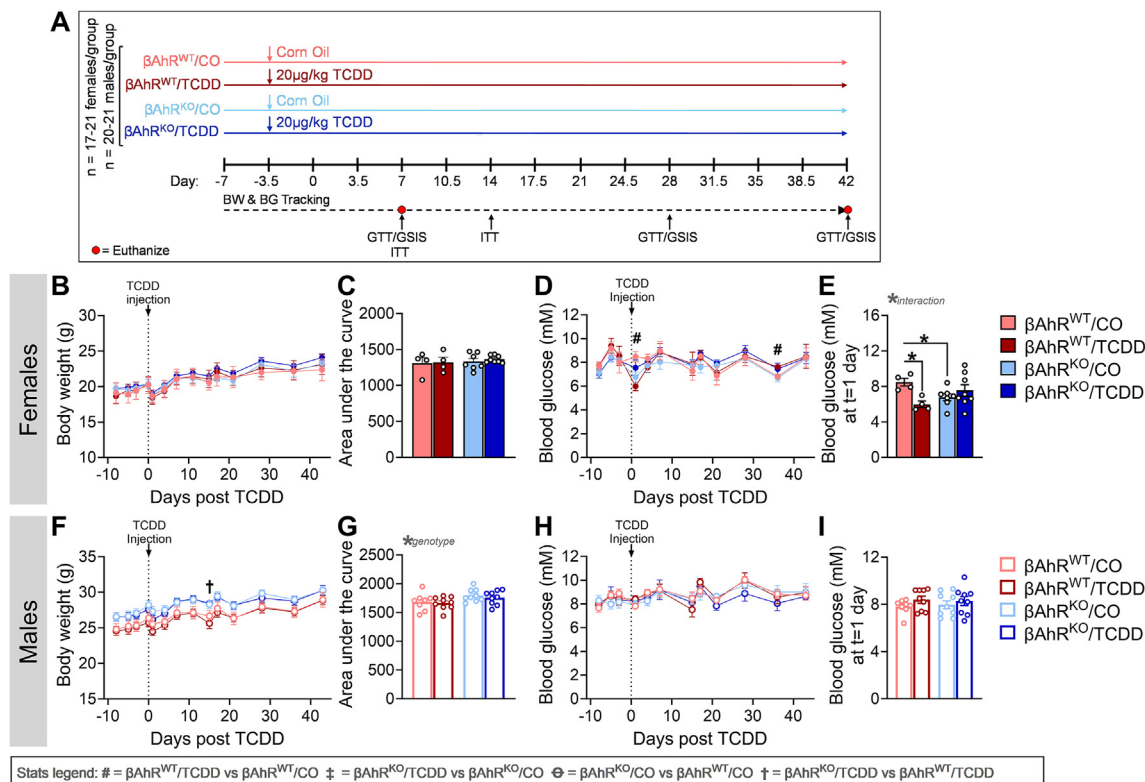


Figure 2: Deletion of *Ahr* from β -cells protected TCDD-exposed female mice from transient hypoglycemia. (A) Schematic summary timeline of the study. Female and male mice were injected with either corn oil (CO) or a single high dose of TCDD (20 μ g/kg) and tracked for up to 6 weeks post CO or TCDD injection. A subset of mice was euthanized at week 1 (n = 11–14/group) and week 6 (n = 4–9/group). BW = body weight, BG = blood glucose, GSIS = glucose-stimulated insulin secretion, GTT = glucose tolerance test, ITT = insulin tolerance test, β Ahr^{WT} = *Ins*^{Cre/+}*Ahr*^{+/+}, β Ahr^{KO} = *Ins*^{Cre/+}*Ahr*^{fl/fl}. (B,C,F,G) Body weight and (D,E,H,I) fasted blood glucose were measured weekly in (B–E) female and (F–I) male mice. (E,I) fasted blood glucose at 1-day post-injection in (E) female and (I) male mice. All data are presented as mean \pm SEM. Individual data points on bar graphs represent biological replicates (different mice). Stats legend ($p < 0.05$): #, β Ahr^{WT}/TCDD vs β Ahr^{WT}/CO; †, β Ahr^{KO}/TCDD vs β Ahr^{KO}/CO; ⊖, β Ahr^{KO}/CO vs β Ahr^{WT}/CO; †, β Ahr^{KO}/TCDD vs β Ahr^{WT}/TCDD. The following statistical tests were used: (B,D,F,H) two-way RM ANOVA with uncorrected Fisher's LSD test; (C,G) two-way ANOVA with Tukey's multiple comparison test; (E,I) two-way ANOVA with uncorrected Fisher's LSD test.

TCDD had no effect on GSIS (Figure 6A,E), stimulation index (Figure 6C,G), or insulin content (Figure 6D,H) in female islets at 1- or 6 weeks post-injection, irrespective of genotype. In contrast, high-dose TCDD exposure *in vivo* significantly impaired *ex vivo* GSIS in β Ahr^{WT} male islets but not β Ahr^{KO} male islets at 1-week post-injection (Figure 6I); GSIS was restored in TCDD-exposed β Ahr^{WT} male islets by 6 weeks post-injection (Figure 6M). TCDD exposure had no effect on stimulation index (Figure 6K,O) or insulin content (Figure 6L,P) in male islets, irrespective of genotype. These data suggest that AhR signaling in β -cells is driving TCDD-induced β -cell dysfunction in males, and likely explains the pronounced hypoinsulinemia in β Ahr^{WT} males *in vivo* following TCDD exposure.

Collectively, our data imply that AhR expression in β -cells plays a role in maintaining basal insulin secretion in female islets under non-chemical conditions. TCDD exposure *in vivo* impairs β -cell function in male but not female β Ahr^{WT} islets, and knocking out β -cell AhR mitigated this effect.

3.7. TCDD exposure increased *I11b* and *Gcg* expression in β Ahr^{WT} but not β Ahr^{KO} islets from female and male mice, respectively

We measured markers of the AhR pathway in isolated islets. At 1-week post-exposure, TCDD caused an overall decrease in *Cyp1a1* in both sexes, irrespective of genotype (Supplemental Figure 2A,D). TCDD also modestly decreased *Ahr* expression in β Ahr^{KO} male islets compared to CO-exposed β Ahr^{KO} islets (Supplemental Figure 2D), indicating

negative feedback regulation of the AhR pathway in islets by 1-week post-injection. Despite the clear loss of *Ahr* in β -cells from our model (Supplemental Figure 1H–I), we only observed a modest downregulation of *Ahr* in CO-exposed β Ahr^{KO} female islets compared to β Ahr^{WT} at 1-week post-exposure (Supplemental Figure 2A), and in β Ahr^{KO} male islets at 6-weeks post-exposure (Supplemental Figure 2E). These data suggest that other endocrine cell types are either compensating for the loss of *Ahr* in β -cells by upregulating *Ahr* expression, or that *Ahr* expression in other islet cells accounts for the majority of total *Ahr* expression in bulk islet samples.

There was no effect of chemical or genotype on *Tnfr* or *Nf-K β* expression in female or male islets (Figure 7A,G), or on *I11b* in male islets (Figure 7G) at 1-week post-injection. At 6 weeks post-injection, we observed a modest increase in *Tnfr* in TCDD-exposed female islets (Supplemental Figure 2C) and a modest decrease in *Nf-K β* in TCDD-exposed male islets, irrespective of genotype (Supplemental Figure 2F). Interestingly, TCDD significantly increased *I11b* expression in β Ahr^{WT} female islets but not β Ahr^{KO} islets at 1-week post-injection (Figure 7A), and this phenotype was not associated with macrophage infiltration into β Ahr^{WT} female islets; we found no F4/80⁺ cells in islets from any treatment group (Supplemental Figure 4). *I11b* expression in TCDD-exposed β Ahr^{WT} female islets was restored by 6 weeks post-injection (Supplemental Figure 2C). Collectively, these data suggest that TCDD-induced AhR activation in β -cells acutely promotes inflammation in female islets.

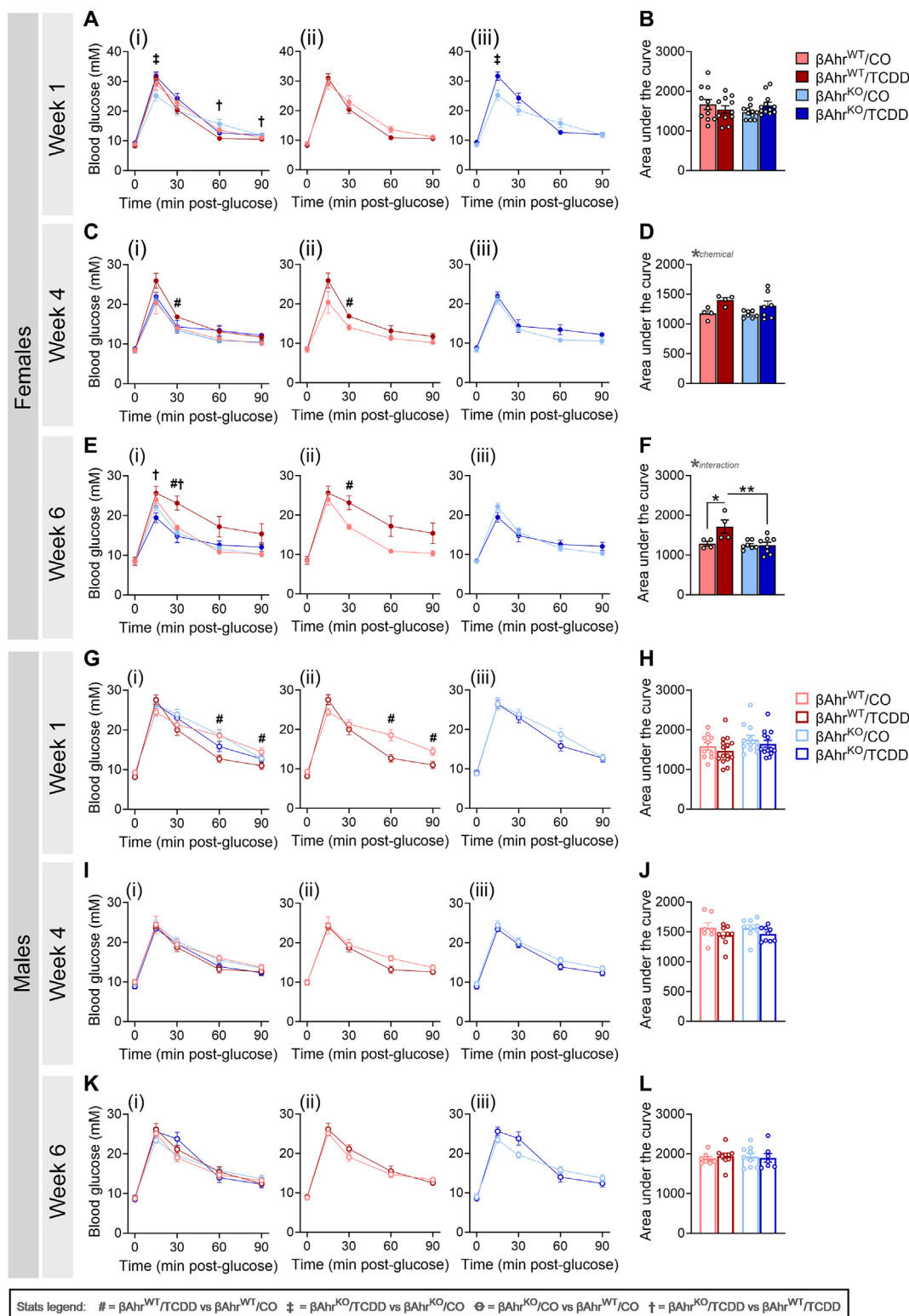


Figure 3: Deletion of *Ahr* in β -cells protected female and male mice from TCDD-induced changes in glycemia. Glucose tolerance tests were performed at (A,B,G,H) 1-week, (C,D,I,J) 4 weeks, and (E,F,K,L) 6 weeks post CO or TCDD injection (see Figure 2A for study timeline). Data is presented as a line graph and area under the curve. Line graphs are presented as (i) all treatment groups, (ii) $\beta\text{Ahr}^{\text{WT}}/\text{TCDD}$ vs $\beta\text{Ahr}^{\text{WT}}/\text{CO}$, and (iii) $\beta\text{Ahr}^{\text{KO}}/\text{TCDD}$ vs $\beta\text{Ahr}^{\text{KO}}/\text{CO}$. All data are presented as mean \pm SEM. Individual data points in bar graphs represent biological replicates (different mice; $n = 4-13$ mice/group). Stats legend ($p \leq 0.05$): #, $\beta\text{Ahr}^{\text{WT}}/\text{TCDD}$ vs $\beta\text{Ahr}^{\text{WT}}/\text{CO}$; ‡, $\beta\text{Ahr}^{\text{KO}}/\text{TCDD}$ vs $\beta\text{Ahr}^{\text{KO}}/\text{CO}$; ⊖, $\beta\text{Ahr}^{\text{KO}}/\text{CO}$ vs $\beta\text{Ahr}^{\text{WT}}/\text{CO}$; †, $\beta\text{Ahr}^{\text{KO}}/\text{TCDD}$ vs $\beta\text{Ahr}^{\text{WT}}/\text{TCDD}$. The following statistical tests were used: line graph, two-way RM ANOVA with uncorrected Fisher's LSD test; bar graphs, two-way ANOVA with Tukey's multiple comparison test.

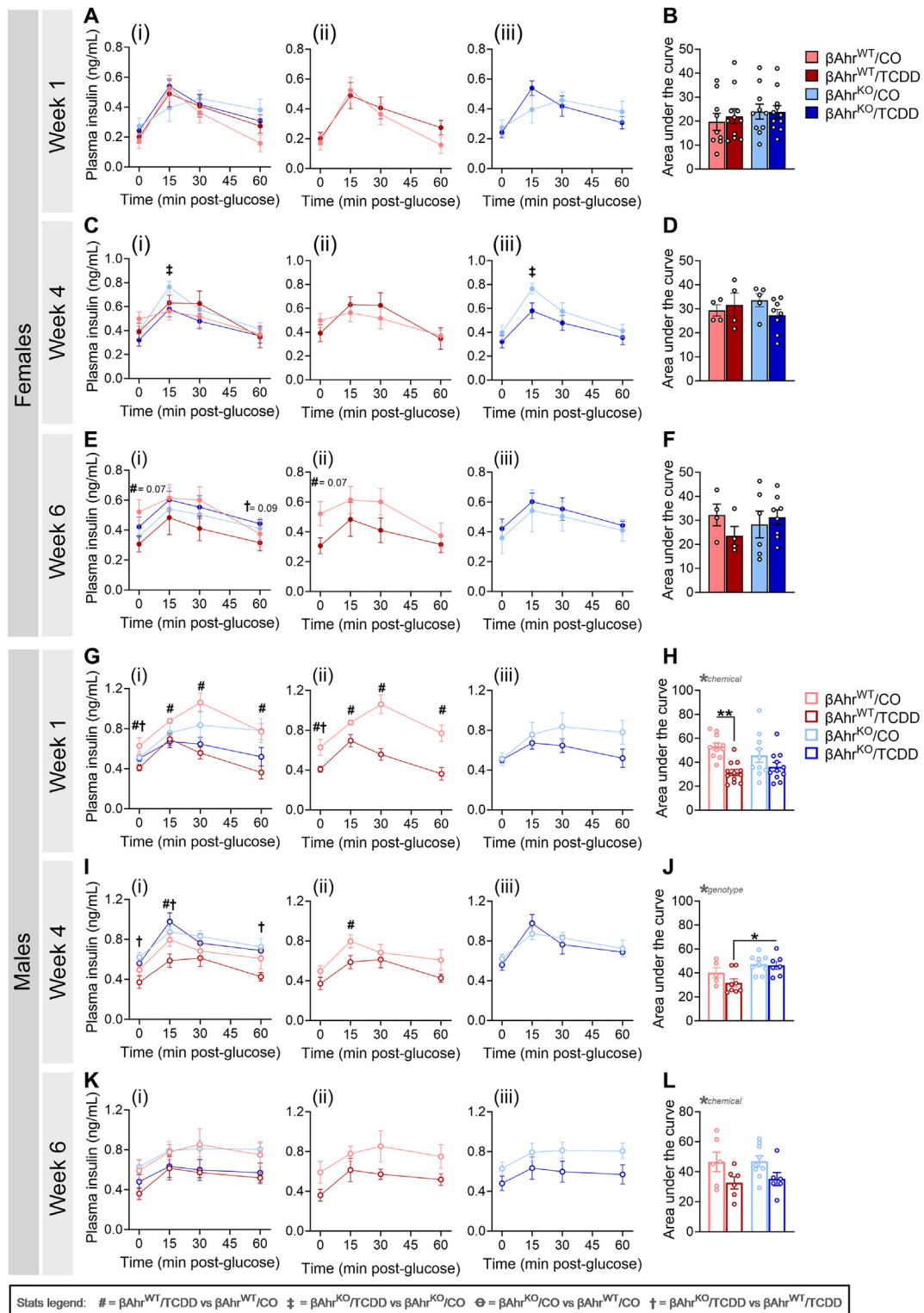


Figure 4: Deleting *Ahr* in β -cells delayed the onset of glucose-induced hypoinsulinemia in TCDD-exposed male mice. Plasma insulin levels were measured during glucose tolerance tests at (A,B,G,H) 1-week, (C,D,I,J) 4 weeks, and (E,F,K,L) 6 weeks post CO or TCDD injection (see Figure 2A for study timeline). Data are presented as a line graph and area under the curve. Line graphs are presented as (i) all treatment groups, (ii) β Ahr^{WT}/TCDD vs β Ahr^{WT}/CO, and (iii) β Ahr^{KO}/TCDD vs β Ahr^{WT}/CO. All data are presented as mean \pm SEM. Individual data points in bar graphs represent biological replicates (different mice; n = 4–12 mice/group). Stats legend (p \leq 0.05): #, β Ahr^{WT}/TCDD vs β Ahr^{WT}/CO; ‡, β Ahr^{KO}/TCDD vs β Ahr^{KO}/CO; ⊕, β Ahr^{KO}/CO vs β Ahr^{WT}/CO; †, β Ahr^{KO}/TCDD vs β Ahr^{WT}/TCDD. The following statistical tests were used: line graph, two-way RM ANOVA with uncorrected Fisher's LSD test; bar graphs, two-way ANOVA with Tukey's multiple comparison test.

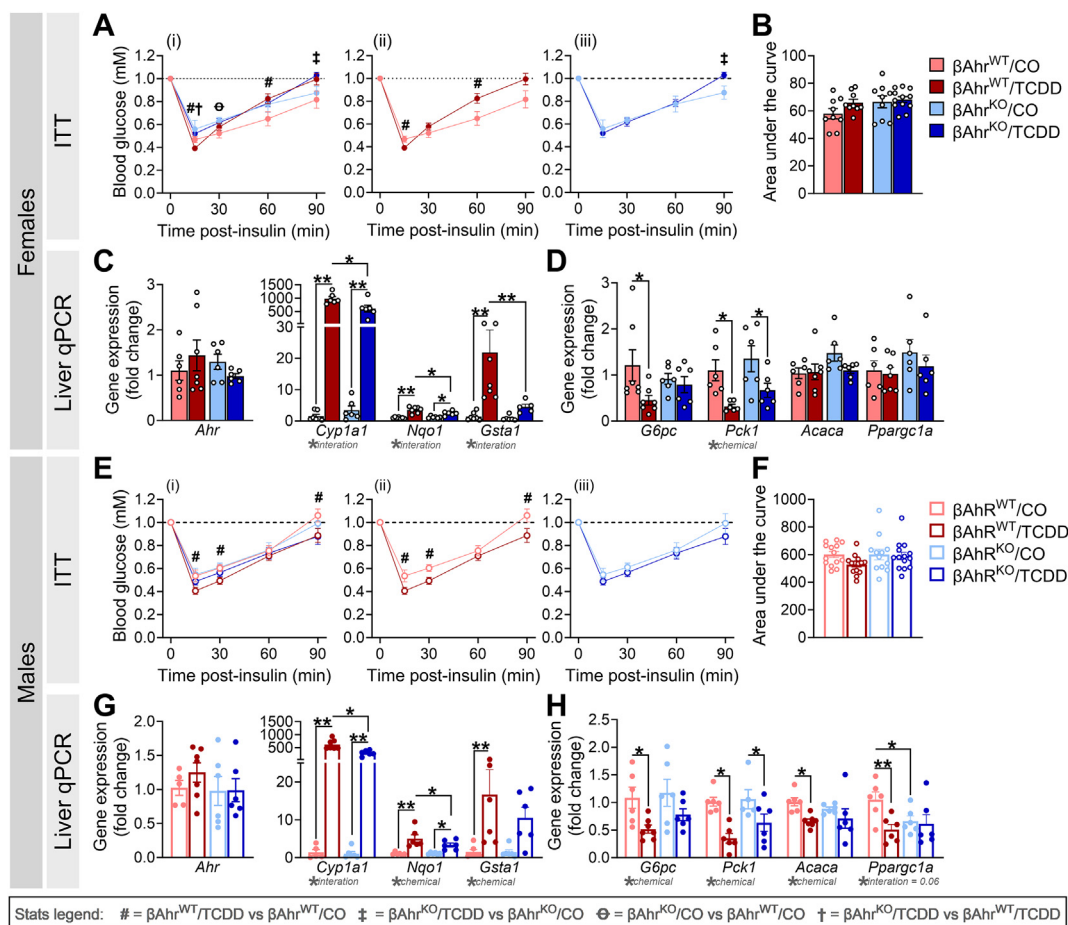


Figure 5: β Ahr^{KO} female and male mice were protected from TCDD-induced changes in insulin sensitivity. An insulin tolerance test (ITT) was performed at 1–2 weeks post CO or TCDD injection, and liver was harvested at 1-week post CO or TCDD injection to assess gene expression by qPCR (see Figure 2A for study timeline). Blood glucose levels during the ITT in (A,B) female and (E,F) male mice (n = 9–14 mice/group). (C,G) Markers of the AhR pathway and (D,H) insulin-dependent markers of gluconeogenesis and lipogenesis in liver from (C,D) female and (G,H) male mice (n = 5–7 mice/group). ITT data is presented as a line graph and area under the curve; line graphs are presented as (i) all treatment groups, (ii) β Ahr^{WT}/TCDD vs β Ahr^{WT}/CO, and (iii) β Ahr^{KO}/TCDD vs β Ahr^{KO}/CO. All data are presented as mean \pm SEM. Individual data points in bar graphs represent biological replicates (different mice). *p \leq 0.05, **p \leq 0.01. Stats legend (p \leq 0.05): #, β Ahr^{WT}/TCDD vs β Ahr^{WT}/CO; ‡, β Ahr^{KO}/TCDD vs β Ahr^{KO}/CO; \ominus , β Ahr^{KO}/CO vs β Ahr^{WT}/CO; †, β Ahr^{KO}/TCDD vs β Ahr^{WT}/TCDD. The following statistical tests were used: (A,E) two-way RM ANOVA with uncorrected Fisher's LSD test; (B,F) two-way ANOVA with Tukey's multiple comparison test; (C,D,G,H) two-way ANOVA with uncorrected Fisher's LSD test.

Next, we assessed whether high-dose TCDD exposure impacted gene expression of islet hormones and markers of β -cell function in β Ahr^{WT} and β Ahr^{KO} mouse islets at 1- and 6 weeks post-injection (Figure 7, Supplemental Figure 3). Despite the pronounced effects of TCDD on glucose homeostasis in β Ahr^{WT} female and male mice, we observed minimal changes in islet gene expression at either time point (Supplemental Figure 3). Most notably, TCDD exposure caused a significant increase in *Gcg* and a decrease in *Gck* in β Ahr^{WT} but not β Ahr^{KO} male islets at 1-week post-injection (Figure 7G); these data align with the hypoinsulinemia observed in TCDD-exposed β Ahr^{WT} but not β Ahr^{KO} males (Figure 4G).

Lastly, we assessed the effects of *in vivo* TCDD exposure on islet cell apoptosis at 1-week post CO or TCDD injection. We did not observe any changes in % live (calcein⁺) (Figure 7B,D,I,J) or % dead (PI⁺) (Figure 7C,D,I,J) cells in dispersed islets of either sex at 1-week post-injection. We also assessed β -cell apoptosis by immunofluorescence staining in pancreas sections at 1-week post-injection and found no changes in % TUNEL^{-ve} INS⁺ cells per islet (Figure 7E,K) or % INS⁺ area per islet (Figure 7F,L) in TCDD-exposed β Ahr^{WT} and β Ahr^{KO} mice of either sex.

4. DISCUSSION

Our study demonstrates that AhR signaling in β -cells plays a role in maintaining metabolic health in mice, even in the absence of exogenous chemical stimuli. β Ahr^{KO} females had modestly reduced fasted blood glucose levels and increased basal and glucose-stimulated insulin secretion *ex vivo*, whereas β Ahr^{KO} males displayed increased body weight compared to β Ahr^{WT} controls. Activation of AhR in β -cells following chemical exposure appears to be detrimental for β -cell health. In line with our previous findings [24], we show that high-dose TCDD exposure has sex-specific effects on glucose homeostasis (summarized in Figure 8). TCDD-exposed β Ahr^{WT} females were more insulin resistant and displayed hyperglycemia during a GTT, and these effects were abolished in TCDD-exposed β Ahr^{KO} females. TCDD-exposed β Ahr^{WT} males showed reduced GSIS *in vivo* and *ex vivo*, increased insulin sensitivity, and hypoglycemia during a GTT, which was also largely mitigated by deleting *Ahr* in β -cells. Importantly, these data imply that AhR signaling in β -cells is not only driving the effects of TCDD on insulin secretion but also on peripheral insulin sensitivity in both sexes. Both loss of AhR (i.e. under baseline conditions) and

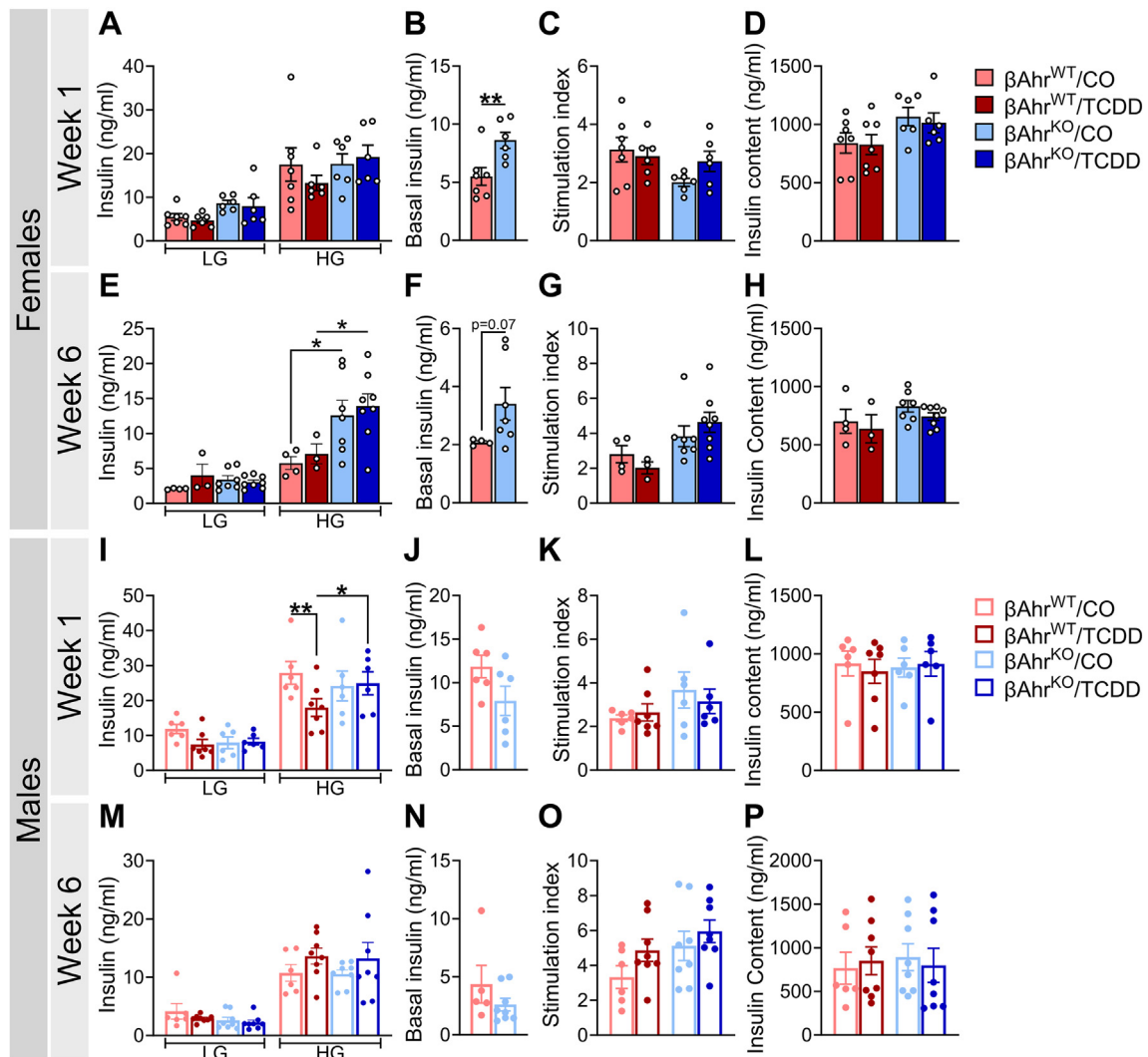


Figure 6: TCDD exposure impaired insulin secretion *ex vivo* in $\beta\text{Ahr}^{\text{WT}}$ but not $\beta\text{Ahr}^{\text{KO}}$ male islets. Islets were isolated at 1- and 6 weeks post CO or TCDD injection to assess islet function *ex vivo* (see Figure 2A for study timeline). LG = low glucose (2.8 mM glucose), HG = high glucose (16.7 mM glucose). (A,E,I,M) Insulin secretion following a sequential 1-h incubation in LG and HG buffer in (A,E) female and (I,M) male islets. (B,F,J,N) Basal insulin secretion following a 1-h incubation in LG buffer in CO-exposed $\beta\text{Ahr}^{\text{WT}}$ and $\beta\text{Ahr}^{\text{KO}}$ (B,F) female and (J,N) male islets. (C,G,K,O) Stimulation index in (C,G) female and (K,O) male islets; stimulation index was calculated as a ratio of insulin concentration under HG relative to LG. (D,H,L,P) Insulin content of islets following an overnight incubation in acid ethanol in (D,H) female and (L,P) male mice. All data are presented as mean \pm SEM. Individual data points in bar graphs represent biological replicates (different mice; $n = 3-8$ mice/group), with each biological replicate representing an average of three technical replicates. * $p < 0.05$, ** $p < 0.01$. The following statistical tests were used: (A,C-E,G-I,K-M,O,P) two-way ANOVA with uncorrected Fisher's LSD test; (B,F,J,N) two-tailed unpaired t-test.

overstimulation of Ahr (i.e. following chemical exposure) in β -cells impairs metabolic health in mice, indicating the importance of this pathway in regulating β -cell physiology. Our study also points to a sex-specific role of Ahr in β -cells.

The main metabolic phenotypes in TCDD-exposed $\beta\text{Ahr}^{\text{WT}}$ female mice were insulin resistance and hyperglycemia, both of which were abolished by deleting *Ahr* in β -cells. Interestingly, TCDD also increased *I1b* expression in islets from $\beta\text{Ahr}^{\text{WT}}$ females but not $\beta\text{Ahr}^{\text{KO}}$ females at 1-week post-injection. We did not observe an increase in macrophage infiltration in TCDD-exposed $\beta\text{Ahr}^{\text{WT}}$ female islets, suggesting that Ahr activation promotes local production of IL-1 β in β -cells, but more detailed analyses are needed to fully assess macrophage accumulation in TCDD-exposed islets. It is well established that elevated IL-1 β signaling in islets leads to β -cell dysfunction and β -cell apoptosis [30–33]. We did not observe an increase in islet cell apoptosis or changes in

% insulin^{+ve} area per islet in female $\beta\text{Ahr}^{\text{WT}}$ mice at 1-week post-TCDD; however, it is plausible that persistent TCDD exposure (and thus, prolonged *I1- β* induction) would lead to β -cell apoptosis. Regardless, deleting *Ahr* in β -cells of female mice prevented the TCDD-induced increase in *I1- β* in islets and onset of glucose intolerance. These data suggest that Ahr-mediated inflammation may contribute to β -cell dysfunction in female mice. Future studies should investigate the interaction between βAhr and the immune system (e.g. inflammasomes).

In line with previous data [24], TCDD-exposed $\beta\text{Ahr}^{\text{WT}}$ males displayed reduced glucose-induced plasma insulin levels, increased insulin sensitivity, and hypoglycemia at 1-week post-injection, which coincided with reduced GSIS *ex vivo*. Past studies have speculated that TCDD alters glucose homeostasis primarily by increasing insulin sensitivity [34–36], which then causes adaptive changes in insulin

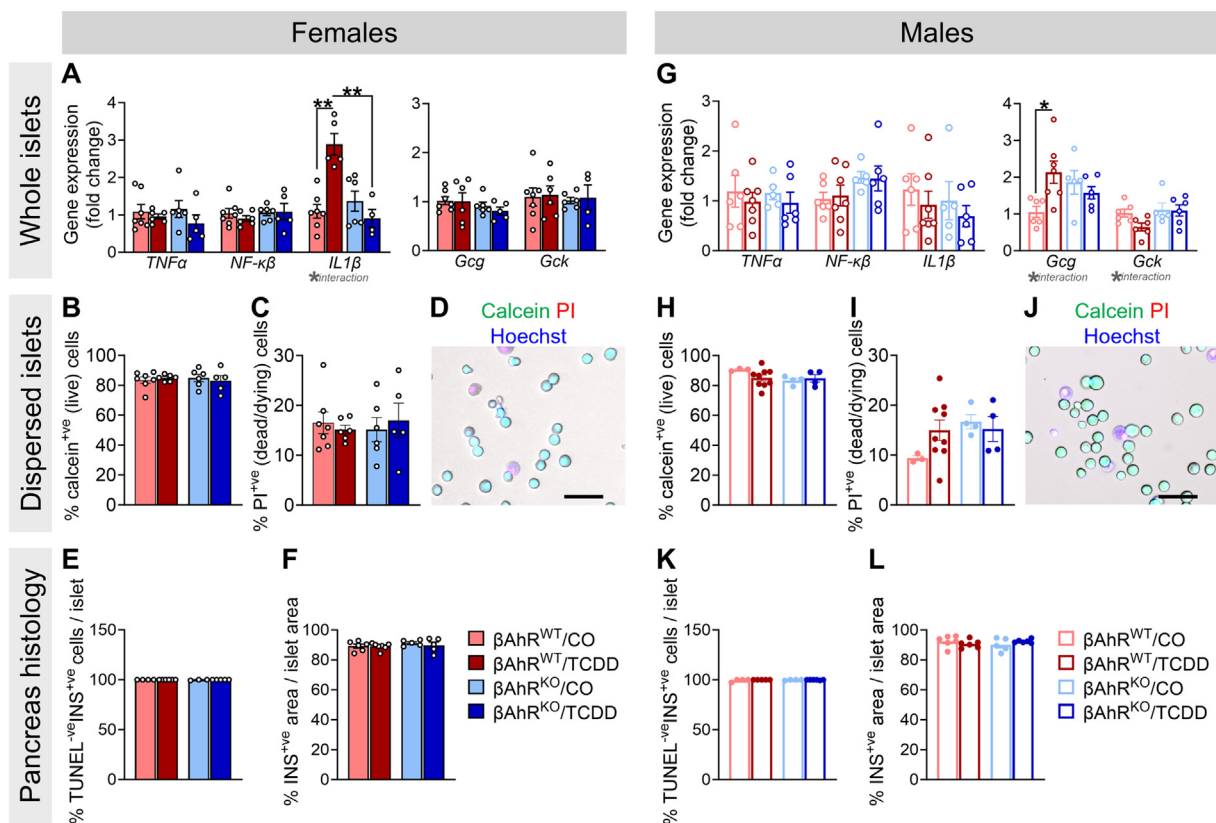










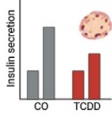



Figure 7: TCDD exposure increased *Il1b* and *Gcg* expression in β Ahr^{WT} but not β Ahr^{KO} islets from female and male mice, respectively. Islets were isolated at 1-week post CO or TCDD injection to assess cell viability and gene expression, and whole pancreas was extracted for histological assessments (see Figure 2A for study timeline). (A,G) Gene expression for inflammatory and β -cell specific markers in (A) female and (G) male islets (n = 5–7 mice/group). (B,H) % calcein⁺ (live) cells and (C,I) % propidium iodide (PI)⁺ (dead/dying) cells in islets from (B,C) female and (H,I) male mice (n = 3–9 mice/group; each mouse is an average of 1–2 technical replicates). (D,J) Representative images showing calcein, PI, and hoechst staining in dispersed islet cells. Scale bar = 50 μ m. (E,K) % TUNEL⁺ insulin (INS)⁺ cells/islet, and (F,L) % INS⁺ area/islet area in pancreas sections from (E,F) female and (K,L) male mice (n = 4–7 mice/group). All data are presented as mean \pm SEM. Individual data points in bar graphs represent biological replicates. *p < 0.05, **p < 0.01. The following statistical tests were used: two-way ANOVA with uncorrected Fisher's LSD test.

secretion. Here we show that deleting *Ahr* in β -cells largely abolished or delayed TCDD-induced metabolic phenotypes in male mice, including changes in peripheral insulin sensitivity. This suggests that β -cell dysfunction is central to the metabolic phenotypes in TCDD-exposed male mice. In line with previous studies, TCDD-exposed β Ahr^{WT} males also had reduced expression of insulin-regulated genes in liver [37–39]; we are the first to provide evidence that these well-documented effects of TCDD in liver are likely driven by changes in insulin secretion (given the absence of these changes in β Ahr^{KO} male liver). Although the mechanisms through which AhR activation impairs β -cell function in male mouse islets remains unclear, we show that TCDD increased *Gcg* (glucagon) and decreased *Gck* (glucokinase; glucose sensor [40]) in islets from β Ahr^{WT} but not β Ahr^{KO} males. These data could point to a role of β Ahr in mediating glucagon secretion from α -cells and/or glucose sensing in β -cells and consequently GSIS. Future studies should consider the role of β Ahr in intra-islet glucagon signaling and glycolysis/glucose metabolism using detailed *ex vivo* perfusion analysis and Seahorse technology.

We provide novel evidence that AhR signaling in β -cells plays a role in maintaining metabolic health in the absence of chemical stimuli. β Ahr^{KO} females had modestly reduced fasting blood glucose levels and increased basal and glucose-stimulated insulin secretion *ex vivo*, suggesting that β Ahr signaling mediates β -cell function in female

mice. However, it is important to note that β Ahr^{KO} females displayed normal fasted and glucose-stimulated plasma insulin levels compared to β Ahr^{WT} females, potentially pointing to increased insulin clearance in β Ahr^{KO} females; more detailed analyses are required to understand this phenotype, including assessing the interaction between β Ahr and sex hormones [41–44]. Interestingly, previous studies report normal fasting blood glucose, fasting c-peptide levels, and glucose tolerance in young global *Ahr*^{KO} female mice (3–4 months of age), but glucose intolerance, hypoinsulinemia, and insulin resistance in aged *Ahr*^{KO} female mice (7–15 months of age) [45,46]. Given that the subset of female mice that were maintained until 6 weeks post-injection in our study were ~3–5 months of age, longer-term studies in older β Ahr^{KO} mice are warranted. We also show that β Ahr^{KO} males displayed increased body weight and reduced hepatic *Pparg1a* expression compared to β Ahr^{WT} controls. *PGC1 α* is a master regulator of mitochondrial biogenesis, fatty acid oxidation, and energy substrate uptake/utilization [47]; *PGC1 α* expression in liver has been negatively correlated with body fat content in humans [47] and liver-specific *PGC1 α* knockout mice display weight gain [48]. As such, our data suggests a baseline role of β -cell AhR signaling in lipid homeostasis and/or body weight regulation. Future studies should characterise changes in fatty acid oxidation and lipid deposition in tissues such as adipose, as well as

| Outcome | FEMALES | | MALES | |
|--|--|---------------------------|--|---|
| | β Ahr ^{WT} | β Ahr ^{KO} | β Ahr ^{WT} | β Ahr ^{KO} |
| GTT  |  BG | X |  BG | X |
| Glucose-induced plasma insulin  |  | X |  |  Delayed |
| ITT  |  BG | X |  BG | X |
| <i>Ex vivo</i> Insulin secretion  | X | X |  | X |

LEGEND:




BG = blood glucose GTT = glucose tolerance test ITT = insulin tolerance test
 = significant increase  = significant decrease  = trending decrease

Figure 8: Metabolic phenotypes in TCDD-exposed β Ahr^{WT} and β Ahr^{KO} mice relative to their CO-exposed genotype controls. Graphical table summarizing the effect of single high-dose TCDD injection on glucose tolerance, glucose-stimulated plasma insulin levels, insulin tolerance, and *ex vivo* β -cell function in female and male β Ahr^{WT} and β Ahr^{KO} mice.

energy expenditure in β Ahr^{KO} mice. It would also be interesting to investigate the role of β -cell AhR signaling in mediating energy homeostasis following HFD feeding.

Our findings in β Ahr^{KO} mice under baseline conditions largely differ from global Ahr^{KO} models. A study by Xu et al. [22] showed that when fed a chow diet, male Ahr^{KO} mice had normal body weight compared to WT mice but were protected from HFD-induced weight gain and hyperinsulinemia. In addition, Wang *et al.* [21] reported that global Ahr^{KO} mice had improved glucose tolerance and increased insulin sensitivity, but no change in glucose-stimulated plasma insulin levels compared to WT mice; note male and female data were pooled in their study. Collectively, studies in global Ahr^{KO} mice suggest that loss of Ahr is protective against metabolic impairments, whereas our study suggests that loss of AhR in β -cells in the absence of a chemical stressor promotes modest weight gain in males and hypersecretion of insulin in females, which could be detrimental. Discrepancies between our data and studies in global Ahr^{KO} mice imply that loss of AhR signaling in β -cells may cause maladaptive AhR-dependent responses in peripheral tissues that are absent in global *Ahr* knockout mice.

Our study provides novel evidence that AhR signaling in β -cells is required for maintaining β -cell function in female mice and body weight in male mice under baseline conditions. Additionally, we show that high-dose TCDD exposure impairs glucose homeostasis and β -cell function via AhR activation in β -cells. This implies that environmental AhR ligands directly target the β -cell and likely contribute to increasing diabetes susceptibility.

CREDIT AUTHORSHIP CONTRIBUTION STATEMENT

Myriam P. Hoyeck: Conceptualization, Data curation, Formal analysis, Investigation, Methodology, Validation, Visualization, Writing — original

draft, Writing — review & editing. **Ma. Enrica Angela Ching:** Investigation. **Lahari Basu:** Investigation. **Kyle van Allen:** Investigation. **Jana Palaniyandi:** Investigation. **Ineli Perera:** Investigation. **Emilia Poleo-Giordani:** Investigation. **Antonio A. Hanson:** Investigation. **Peyman Ghorbani:** Investigation. **Morgan D. Fullerton:** Funding acquisition, Resources. **Jennifer E. Bruin:** Conceptualization, Data curation, Formal analysis, Funding acquisition, Investigation, Methodology, Project administration, Resources, Supervision, Validation, Visualization, Writing — original draft, Writing — review & editing.

ACKNOWLEDGEMENTS

We thank Dr. Erin Mulvihill (Ottawa Heart Research Institute) and Dr. Søs Scovø (Valkyrie Life Sciences) for helpful discussions about Cre-LoxP breeding schemes. This research was supported by a Canadian Institutes of Health Research (CIHR) Project Grant (#PJT-2018-159590 to J.E.B. and #PJT-2020-148634 to M.D.F.), a Diabetes Canada operating grant (OG-3-22-5657-to M.D.F.), the Canadian Foundation for Innovation John R. Evans Leaders Fund (#37231 to J.E.B.), and an Ontario Research Fund award (to J.E.B.). M.P.H. was supported by a CIHR CGS-D award. M.E.A.C. was supported by an NSERC CGS-M and NSERC CGS-D award. L.B. was supported by an CIRTN-R2FIC-CREATE and CIHR CGS-D award. M.D.F. holds a Camille Villeneuve Chair in Cardiovascular Immunometabolism and J.E.B. is supported by an Early Researcher Award from the Ontario Government.

DECLARATION OF COMPETING INTEREST

The authors declare that they have no known competing financial interests or personal relationships that could have appeared to influence the work reported in this paper.

DATA AVAILABILITY

Data will be made available on request.

APPENDIX A. SUPPLEMENTARY DATA

Supplementary data to this article can be found online at <https://doi.org/10.1016/j.molmet.2024.101893>.

REFERENCES

- [1] Hoyeck MP, Matteo G, MacFarlane EM, Perera I, Bruin JE. Persistent organic pollutants and β -cell toxicity: a comprehensive review. *Am J Physiol Endocrinol Metab* 2022;322(5):E383–413. <https://doi.org/10.1152/ajpendo.00358.2021>.
- [2] Thayer KA, Heindel JJ, Bucher JR, Gallo MA. Role of environmental chemicals in diabetes and obesity: a national toxicology program workshop review. *Environ Health Perspect* 2012;120(6):779–89. <https://doi.org/10.1289/ehp.1104597>.
- [3] Taylor KW, Novak RF, Anderson HA, Birnbaum LS, Blystone C, Devito M, et al. Evaluation of the association between persistent organic pollutants (POPs) and diabetes in epidemiological studies: a national toxicology program workshop review. *Environ Health Perspect* 2013;121(7):774–83. <https://doi.org/10.1289/ehp.1205502>.
- [4] Lee Duk-Hee, Porta M, Jacobs Jr David R, Vandenberg LN. Chlorinated persistent organic pollutants, obesity, and type 2 diabetes. *Endocr Rev* 2014;35:557–601. <https://doi.org/10.1210/er.2013-1084>.
- [5] Sun W, Clark JM, Park Y. Environmental pollutants and type 2 diabetes: a review of human studies. *Toxicology & Environmental Chemistry* 2017;99(9–10):1283–303. <https://doi.org/10.1080/02772248.2017.1393818>.
- [6] Ngwa EN, Kengne A-P, Tiedeu-Atogho B, Mofo-Mato E-P, Sobngwi E. Persistent organic pollutants as risk factors for type 2 diabetes. *Diabetol Metab Syndrom* 2015;7(1):41. <https://doi.org/10.1186/s13098-015-0031-6>.
- [7] Roth K, Petriello MC. Exposure to per- and polyfluoroalkyl substances (PFAS) and type 2 diabetes risk. *Front Endocrinol* 2022;13:965384. <https://doi.org/10.3389/fendo.2022.965384>.
- [8] Chen HL, Su HJ, Guo YL, Liao PC, Hung CF, Lee CC. Biochemistry examinations and health disorder evaluation of Taiwanese living near incinerators and with low serum PCDD/Fs levels. *Sci Total Environ* 2006;366(2–3):538–48. <https://doi.org/10.1016/j.scitotenv.2005.11.004>.
- [9] Dirinck EL, Dirtu AC, Govindan M, Covaci A, Van Gaal LF, Jorens PG. Exposure to persistent organic pollutants: relationship with abnormal glucose metabolism and visceral adiposity. *Diabetes Care* 2014;37(7):1–8. <https://doi.org/10.2337/dc13-2329>.
- [10] Raafat N, Abass MA, Salem HM. Malathion exposure and insulin resistance among a group of farmers in Al-Sharkia governorate. *Clin Biochem* 2012;45(18):1591–5. <https://doi.org/10.1016/j.clinbiochem.2012.07.108>.
- [11] Cordier S, Anassour-Laouan-Sidi E, Lemire M, Costet N, Lucas M, Ayotte P. Association between exposure to persistent organic pollutants and mercury, and glucose metabolism in two Canadian Indigenous populations. *Environ Res* 2020;184(November 2019):109345. <https://doi.org/10.1016/j.envres.2020.109345>.
- [12] Grandjean P, Henriksen JE, Choi AL, Petersen MS, Dalgård C, Nielsen F, et al. Marine food pollutants as a risk factor for hypoinsulinemia and type 2 diabetes. *Epidemiology* 2011;22(2):410–7. <https://doi.org/10.1097/EDE.0b013e318212fab9>.
- [13] Jørgensen ME, Borch-Johnsen K, Bjerregaard P. A cross-sectional study of the association between persistent organic pollutants and glucose intolerance among Greenland Inuit. *Diabetologia* 2008;51(8):1416–22. <https://doi.org/10.1007/s00125-008-1066-0>.
- [14] Lee YM, Ha CM, Kim SA, Thoudam T, Yoon YR, Kim DJ, et al. Low-dose persistent organic pollutants impair insulin secretory function of pancreatic β -cells: human and in vitro evidence. *Diabetes* 2017;66(10):2669–80. <https://doi.org/10.2337/db17-0188>.
- [15] Dietrich C. Antioxidant functions of the aryl hydrocarbon receptor. *Stem Cell Int* 2016;2016:7943495. <https://doi.org/10.1155/2016/7943495>.
- [16] Larigot L, Juricek L, Dairou J, Coumoul X. AhR signaling pathways and regulatory functions. *Biochimie Open* 2018;7:1–9. <https://doi.org/10.1016/j.biopen.2018.05.001>.
- [17] Barouki R, Coumoul X, Fernandez-Salguero PM. The aryl hydrocarbon receptor, more than a xenobiotic-interacting protein. *FEBS (Fed Eur Biochem Soc) Lett* 2007;581(19):3608–15. <https://doi.org/10.1016/j.febslet.2007.03.046>.
- [18] Kou Z, Dai W. Aryl hydrocarbon receptor: its roles in physiology. *Biochem Pharmacol* 2021;185:114428. <https://doi.org/10.1016/j.bcp.2021.114428>.
- [19] Lamas B, Natividad JM, Sokol H. Aryl hydrocarbon receptor and intestinal immunity. *Mucosal Immunol* 2018;11(4):1024–38. <https://doi.org/10.1038/s41385-018-0019-2>.
- [20] Gutiérrez-Vázquez C, Quintana FJ. Regulation of the immune response by the aryl hydrocarbon receptor. *Immunity* 2018;48(1):19–33. <https://doi.org/10.1016/j.immuni.2017.12.012>.
- [21] Wang C, Xu C-X, Krager SL, Bottum KM, Liao D-F, Tischkau SA. Aryl hydrocarbon receptor deficiency enhances insulin sensitivity and reduces PPAR- α pathway activity in mice. *Environ Health Perspect* 2011;119(12):1739–44. <https://doi.org/10.1289/ehp.1103593>.
- [22] Xu C-X, Wang C, Zhang Z-M, Jaeger CD, Krager SL, Bottum KM, et al. Aryl hydrocarbon receptor deficiency protects mice from diet-induced adiposity and metabolic disorders through increased energy expenditure. *Int J Obes* 2015;39(8):1300–9. <https://doi.org/10.1038/ijo.2015.63> (2005).
- [23] Ibrahim M, MacFarlane EM, Matteo G, Hoyeck MP, Rick KRC, Boroujeni SF, et al. Functional cytochrome P450 1a enzymes are induced in mouse and human islets following pollutant exposure. *Diabetologia* 2020;63:162–78. <https://doi.org/10.1007/s00125-019-05035-0>.
- [24] Hoyeck MP, Blair H, Ibrahim M, Solanki S, Elsayy M, Prakash A, et al. Long-term metabolic consequences of acute dioxin exposure differ between male and female mice. *Sci Rep* 2020;10(1):1448. <https://doi.org/10.1101/762476>.
- [25] Matteo G, Hoyeck M, Blair H, Zebarth J, Rick K, Williams A, et al. Prolonged low-dose dioxin exposure impairs metabolic adaptability to high-fat diet feeding in female but not male mice. *Endocrinology* 2021;162(6):bqab050. <https://doi.org/10.1210/endo/bqab050>.
- [26] Kurita H, Yoshioka W, Nishimura N, Kubota N, Kadowaki T, Tohyama C. Aryl hydrocarbon receptor-mediated effects of 2,3,7,8-tetrachlorodibenzo-p-dioxin on glucose-stimulated insulin secretion in mice. *J Appl Toxicol* 2009;29(8):689–94. <https://doi.org/10.1002/jat.1459>.
- [27] Berthault C, Staels W, Scharfmann R. Purification of pancreatic endocrine subsets reveals increased iron metabolism in beta cells. *Mol Metab* 2020;42:101060. <https://doi.org/10.1016/j.molmet.2020.101060>.
- [28] Mehran AE, Templeman NM, Brigidi GS, Lim GE, Chu K-Y, Hu X, et al. Hyperinsulinemia drives diet-induced obesity independently of brain insulin production. *Cell Metab* 2012;16(6):723–37. <https://doi.org/10.1016/j.cmet.2012.10.019>.
- [29] Templeman NM, Flibotte S, Chik JHL, Sinha S, Lim GE, Foster LJ, et al. Reduced circulating insulin enhances insulin sensitivity in old mice and extends lifespan. *Cell Rep* 2017;20(2):451–63. <https://doi.org/10.1016/j.celrep.2017.06.048>.
- [30] Alfadul H, Sabico S, Al-Daghri NM. The role of interleukin-1 β in type 2 diabetes mellitus: a systematic review and meta-analysis. *Front Endocrinol* 2022;13.
- [31] Böni-Schnetzler M, Méreau H, Rachid L, Wiedemann SJ, Schulze F, Trimiglozzi K, et al. IL-1 β promotes the age-associated decline of beta cell function. *iScience* 2021;24(11):103250. <https://doi.org/10.1016/j.isci.2021.103250>.

- [32] Böni-Schnetzler M, Donath MY. Increased IL-1 β activation, the culprit not only for defective insulin secretion but also for insulin resistance? *Cell Res* 2011;21(7):995–7. <https://doi.org/10.1038/cr.2011.85>.
- [33] Böni-Schnetzler M, Häuselmann SP, Dalmas E, Meier DT, Thienel C, Traub S, et al. β cell-specific deletion of the IL-1 receptor antagonist impairs β cell proliferation and insulin secretion. *Cell Rep* 2018;22(7):1774–86. <https://doi.org/10.1016/j.celrep.2018.01.063>.
- [34] Kern PA, Said S, Jackson WG, Michalek JE. Insulin sensitivity following Agent Orange exposure in Vietnam veterans with high blood levels of 2,3,7,8-tetrachlorodibenzo-p-dioxin. *J Clin Endocrinol Metab* 2004;89(9):4665–72. <https://doi.org/10.1210/jc.2004-0250>.
- [35] Chang JW, Chen HL, Su HJ, Liao PC, Guo HR, Lee CC. Dioxin exposure and insulin resistance in Taiwanese living near a highly contaminated area. *Epidemiology* 2010;21:56–61. <https://doi.org/10.1097/EDE.0b013e3181c2fc6e>.
- [36] Fried KW, Guo GL, Esterly N, Kong B, Rozman KK. 2,3,7,8-tetrachlorodibenzo-p-dioxin (TCDD) reverses hyperglycemia in a type II diabetes mellitus rat model by a mechanism unrelated to PPAR γ . *Drug Chem Toxicol* 2010;33(3):261–8. <https://doi.org/10.3109/01480540903390026>.
- [37] Fader KA, Nault R, Doskey CM, Fling RR, Zacharewski TR. 2,3,7,8-Tetrachlorodibenzo-p-dioxin abolishes circadian regulation of hepatic metabolic activity in mice. *Sci Rep* 2019;9:6514. <https://doi.org/10.1038/s41598-019-42760-3>.
- [38] Boverhof DR, Burgoon LD, Tashiro C, Chittim B, Harkema JR, Jump DB, et al. Temporal and dose-dependent hepatic gene expression patterns in mice provide new insights into TCDD-mediated hepatotoxicity. *Toxicol Sci* 2005;85(2):1048–63. <https://doi.org/10.1093/toxsci/kfi162>.
- [39] Forgacs AL, Kent MN, Makley MK, Mets B, DelRaso N, Jahns GL, et al. Comparative metabolomic and genomic analyses of TCDD-elicited metabolic disruption in mouse and rat liver. *Toxicol Sci* 2012;125(1):41–55. <https://doi.org/10.1093/toxsci/kfr262>.
- [40] Matschinsky FM, Wilson DF. The central role of glucokinase in glucose homeostasis: a perspective 50 Years after demonstrating the presence of the enzyme in islets of langerhans. *Front Physiol* 2019;10.
- [41] Nadal A, Alonso-Magdalena P, Soriano S, Quesada I, Ropero AB. The pancreatic beta-cell as a target of estrogens and xenoestrogens: implications for blood glucose homeostasis and diabetes. *Mol Cell Endocrinol* 2009;304(1–2):63–8. <https://doi.org/10.1016/j.mce.2009.02.016>.
- [42] Gargaro M, Scalisi G, Manni G, Mondanelli G, Grohmann U, Fallarino F. The landscape of AhR regulators and coregulators to fine-tune AhR functions. *Int J Mol Sci* 2021;22(2). <https://doi.org/10.3390/ijms22020757>.
- [43] Matthews J, Gustafsson J-Å. Estrogen receptor and aryl hydrocarbon receptor signaling pathways. *Nucl Recept Signal* 2006;4:e016. <https://doi.org/10.1621/nrs.04016>.
- [44] Tramunt B, Smati S, Grandgeorge N, Lenfant F, Arnal J-F, Montagner A, et al. Sex differences in metabolic regulation and diabetes susceptibility. *Diabetologia* 2019. <https://doi.org/10.1007/s00125-019-05040-3>.
- [45] Thackaberry EA, Bedrick EJ, Goens MB, Danielson L, Lund AK, Gabaldon D, et al. Insulin regulation in AhR-null mice: embryonic cardiac enlargement, neonatal macrosomia, and altered insulin regulation and response in pregnant and aging AhR-null females. *Toxicol Sci* 2003;76(2):407–17. <https://doi.org/10.1093/toxsci/kfg229>.
- [46] Biljes D, Hammerschmidt-Kamper C, Kadow S, Diel P, Weigt C, Burkart V, et al. Impaired glucose and lipid metabolism in ageing aryl hydrocarbon receptor deficient mice. *EXCLI Journal* 2015;14:1153–63. <https://doi.org/10.17179/excli2015-638>.
- [47] Morris EM, Meers GME, Booth FW, Fritsche KL, Hardin CD, Thyfault JP, et al. PGC-1 α overexpression results in increased hepatic fatty acid oxidation with reduced triacylglycerol accumulation and secretion. *Am J Physiol Gastrointest Liver Physiol* 2012;303(8):G979–92. <https://doi.org/10.1152/ajpgi.00169.2012>.
- [48] Besse-Patin A, Léveillé M, Oropeza D, Nguyen BN, Prat A, Estall JL. Estrogen signals through peroxisome proliferator-activated Receptor- γ coactivator 1 α to reduce oxidative damage associated with diet-induced fatty liver disease. *Gastroenterology* 2017;152(1):243–56. <https://doi.org/10.1053/j.gastro.2016.09.017>.